25th ABCM International Congress of Mechanical Engineering
October 20-25, 2019, Uberlândia, MG, Brazil

# A STUDY ON THE KINEMATICS AND DYNAMICS OF FLAGELLUM MOTION IN CREEPING FLOWS.

**Yves-Garnard IRILAN**
**Francisco Ricardo CUNHA**
UNIVERSIDADE DE BRASILIA
irilanyvesgar@yahoo.fr - frcunha2@gmail.com

***Abstract.*** *The low Reynold number flow around micro-organism (e.g bacteria, algae ) has captivated the interest of many scientists. For these micro-organisms Reynold's number is less than one, meaning viscous effects are dominant and inertial forces are insignificant. Bacteria propel themselves in aqueous environment by rotating helically shaped flagella. Many theoretical and experimental works have been done to date, however propulsion by helical flagellum is a major challenge due to the complexity of tracking the movement of the head and body of the flagellum. In the present study, a biomimetic swimmer, which propels itself by mimicking the helical flagella motion of micro-organism, is developed. First, we apply the Slender Body Theory (SBT) in order to describe the dynamics of swimming micro-organism with motion produced by helical flagellum propulsion. Numerical simulations are performed based on resistive force theories. In addition, we carried out some experiments with a macroscopic prototype micro-organisms in creeping flow motion. Silicon oil is used in order to ensure a low Reynolds number around the particle. The propulsive velocity, angular velocity and propulsive thrust and torque are measured in the experiments and they are also compared with those predicted using numerical simulation. The predictions form Resistive Force Theory are found to be in very good agreement with the experimental observation of our artificial flagellum.*
***Keywords:*** *Low Reynolds number flow, Resistive Force Theory , Helical flagellum*

## 1. INTRODUCTION

The study of the locomotion of self propelled organisms has attracted the interest of the scientific community in the last five decades in order to understand the physics behind this phenomenon. In addition, another issue of interest is to understand how this locomotion affects biological processes such as reproduction human or bacterial infection. These investigations have also prompted the creation of artificial micro-swimmers. While some synthetic devices have been designed to prove theoretical models. More recently, a practical application is to study the motion of micro-organism in creeping flow in order to design nano and micro-robots. Micro-robots can make a great impact in medical applications such as minimally-invasive surgery, screening and diagnosis of diseases, targeted therapy and drug delivery. Small-sized bio-inspired robots can mimic flagellar propulsion mechanisms of micro-organisms for actuation in microfluidic environments, which are dominated by viscous forces. In fluid mechanics, slender-body theory is a methodology that can be used to take advantage of the slenderness of a body to obtain an approximation to a field surrounding it and/or the net effect of the field on the body. Several applications are explored for the condition of Stokes flow where the micro-organism needs to break the time reversibility imposed by the creeping around it. For a helical flagellum the theory was first elaborated by Gray and Hancock (1955) and later it was improved by Lighthill (1976). Liu et al (2011) measured the force-free velocity of a rotating rigid propeller immersed in viscous and visco-elastic fluids at low Reynolds numbers as a function of geometry and propeller rotation rate. The propeller was introduced into the fluid by rotating at angular velocity $W$ and a constant velocity $V$ in a tank filled with a visco-elastic fluid or a newtonian fluid. Kock (2011) explore simulations of hydrodynamically interacting self-propelled particles as well as stability analyses and numerical solutions of averaged equations of motion for low Reynolds number swimmers. It has been found that spontaneous motions can arise in such systems from the coupling between the stresses the bacteria induce in the fluid as they swim and the rotation of the bacteria due to the resulting fluid velocity disturbances. In this work, we implement a code for describing the motion of a thin flagellum undergoing a creeping flow. Specifically, this work has used the so-called Resistive Force Theory (RFT) based on drag coefficients as described in the available literature by Johnson (1980). A biomimetic swimmer, which propels itself using the helical flagella swimming technique, is developed in this work. In addition we carry out some experiments with a macroscopic model who swim freely in a silicone oil bath in order to ensure a low Reynolds number around the particle. In this preliminary studies the idea is understand the mechanics of a artifitial swimming moving with a small Reynolds number in a viscous flow. With this end we have analysed the falgellum oscillatory motion. We characterize

the dynamics of the flagellum motion and calculate the force and torque acting on the micro-organisms as a function of its wavelength and the main physical parameters of the problem. The propulsion velocity of the micro-organism is already examined for the ambient in the viscous fluid. In addition, characteristics of the macro flagellum is explored experimentally and compared with our RST simulation results.

## 2. EXPERIMENTAL SET-UP

In order to check the validity of the developed theories, an experimental setup is constructed to measure the thrust force and torque produced by a single artificial flagellum at Reynolds numbers comparable to those of real micro-organisms. The experiments are carried out in a rectangular-tank (150 mm x 150 mm x 200 mm high) filled with silicone oil. The tank dimensions and the area of interest for the run is chosen such that the head is away from the side walls by about 35 mm, and the free surface (top) by about 45 mm. The viscosity was measured using a parallel disk rheometer with a controlled gap. The flagellum has two components head and tail. The head is made from glass tube and a small DC motor, (vibracall-drone motor ) it is housed inside the head. The helical tail of the swimmer is made of steel wires wrapped around mandrels with helical V-shaped. Three different helices was used for these experiments, the parameters are given in table 1.

| Parameters | Helix 1 | Helix 2 | Helix 3 |
|---|---|---|---|
| Wavelength($\lambda$)[mm] | $1.82 \pm 0.05$ | $6.14 \pm 0.05$ | $9.92 \mp 0.05$ |
| Number of turn($N$) | 11 | 6 | 4 |
| Helical Radius ($R$)[mm] | $4.50 \pm 0.05$ | $2.7 \pm 0.05$ | $2 \pm 0.05$ |

Table 1. Typical dimensional parameters for the experiment

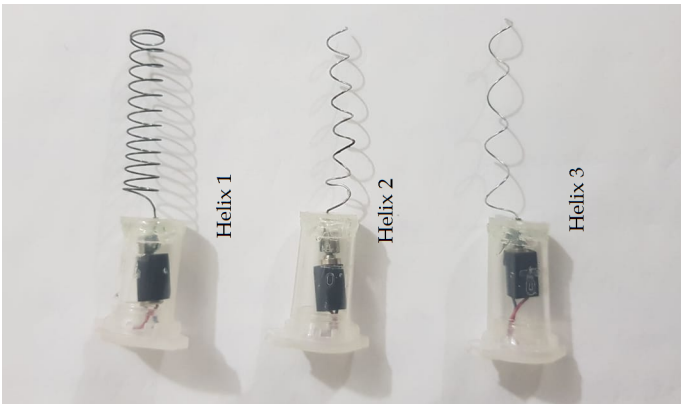


Figure 1. Schematic of the prototypes: helix 1, helix 2, helix 3.

The prototypes developed in the present work is shown in figure 1 and figure 2 shown the schematic of helical flagellum with the parameters. $R$ is the helix radius, $a$ is the filament radius, $\theta$ the pitch angle, $L$ axial length and $\lambda$ the wavelength. The schematic of the experimental setup is shown in figure 3.

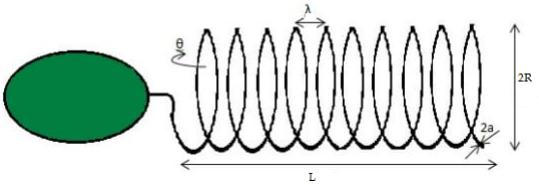


Figure 2. Schematic of geometrical parameters

### 2.1 Experimental Method

As explained above, in order to experimentally quantify the propulsive characteristics of the design, we built a robotic swimmer. The flagellum is placed in vertical direction on the test-bench, at the center of the rectangular tank. First, we carried out a buoyancy test, in this test the flagellum is placed in fluid with the motor turned off. Adjustments are made adding small spheres, then the weight of the flagellum is balanced with the fluid. In this case it stays in the same place

inside the tank by a long period. Measurements of the force and torque is done using sensors. The thrust measurement was performed using a calibrated load cell. The load cell using here is an electronic accessory capable to detecting different loads that are on its half-bridge, however for operation it must act in conjunction with a arduino. On the center of the load cell there is a sensitive area responsible for detecting the load. Electrically, when the weight of the flagellum is applied, it sends a voltage to the microcontroller. It is important to remember that the voltage is so low that we use a signal amplifier for communication with the arduino. Transducer is used to create an electrical signal whose magnitude is directly proportional to the force of the swimmer. Our system do the interfacing HX711 load cell amplifier with arduino and we measure the thrust generated by the rotating flagellum. The propulsive force induced by the helix was obtained from the difference between the average force measured at the motor turned off position and the running position in the silicone oil after six minutes. The torque measurement system used is a calibrated 6mm Speed Sensor also called optical sensor or counting sensor. The main function of the 6mm speed sensor is to perform the reading of encoder disks, as it counts an emitter and an infrared receiver at its ends, which serve to define the speed of movement of the flagellum. However, for this information to be recognized by the user, the presence of the arduino Speed Sensor 6mm for encoder disks is used and is possible to estimate the speed or rotation of the flagellum. The arduino emits a beam of infrared light imperceptible to human vision, when this beam is broken by the stripes or perforations of the encoder disk, the microcontroller system programmed, will be aware speed and position of movement for the microswimmer. The fluid was mixed thoroughly to avoid temperature variation or density stratification in the tank, and the experiments will started after ensuring that the convection currents and bubbles generated during mixing are eliminated. The swimming robot is placed inside the box and we use an external DC power to provide the rotational frequency of the motor as we can see in figure 3. The difference in the weights of the model when the motor is running and when the motor is switched off is taken as a measure of the thrust force produced by the rotating tail. This is done for all the helical tails and the values obtained are recorded. This method allows the thrust to be measured without interfering with the free movement of the swimmer. With the sensors describe early we recorded the thrust force and torque by the rotating helix on the surrounding fluid. In this experiment the weight of the model can be measured with an accuracy of 0.05 gram. The experiment was repeated 4 times for each case and an average over the experimental run was determined in order to perform the plots presented. In all experiments we obtain the force and the torque on the swimmer also the flagellum angular velocity and consequently the propulsion velocity. The frequency was recorded at interval of 5 minutes.

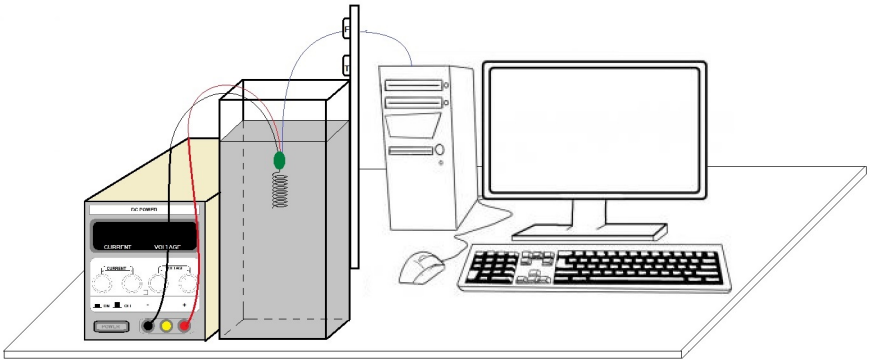

Figure 3. Sketch of the experimental set-up to investigate the model of a flagellum motion in creeping flow

## 3. Theoretical And Numerical Model

For creeping flows of an incompressible Newtonian fluid the motion is governed by:

$$\begin{cases} \nabla \cdot \mathbf{u} = 0 \\ \rho \dfrac{\partial \mathbf{u}}{\partial t} = -\nabla p + \mu \nabla^2 \mathbf{u} \end{cases} \tag{1}$$

In equation (1), $\mathbf{u}(\mathbf{x}, t)$ denotes the Eulerian velocity of the fluid at $\mathbf{x}$ in space and time $t$, $\mu$ represent the viscosity of the fluid, $\rho$ is the density of the fluid and $p$ is the pressure. Now, if $\delta$ is a typical micro-organism length scale and $U_0$ a characteristic velocity of the particle motion like $\lambda\ f$, where $\lambda$ and $f$ are the wavelength and the frequency of the flagellum, respectively, the Reynolds number $Re$ can be evaluated as $Re = \rho\delta\lambda f/\mu$ that is considered much smaller than unit. Considering $\delta \sim \lambda$ we ave then $Re = \rho\lambda^2 f/\mu << 1$.

For Stokes flows, the solution of equation (1) with the appropriated boundary conditions can be represented in therm of a Resistance Formulation Kim and Karrila (1991). Actually, we solve the reduced flagellum rotating and translating in

the axial direction (i.e. bacterial swimming). By the Resistance formulation the force and torque on the active particle in the x-direction, $F_x$ and $T_x$, are determines in terms of the translational and rotational velocity of the particle in $U$ and $\omega$. The resistance formulation is expressed as follows:

$$\begin{pmatrix} \mathbf{F} \\ \mathbf{T} \end{pmatrix} = \begin{pmatrix} \mathbf{A} & \mathbf{B} \\ \mathbf{C} & \mathbf{D} \end{pmatrix} \begin{pmatrix} \mathbf{U} \\ \omega \end{pmatrix} \tag{2}$$

The matrix in equation (2) is referred to as the Grand (resistance) matrix and all elements of this mobility functions depend only on the geometry of the flagellum. The sub-matrices $\mathbf{A}$, $\mathbf{B}$ and $\mathbf{C}$ are three-dimensional and symmetric and therefore, so is the entire resistance matrix. If this matrix is known, the trajectory of the helical flagellum can be fully determined. As in this work we focus on some kinematic properties and the calculations of force and torque on the active flagellum-micro-organism, the calculation of the particle stresslet is not considered in this stage. We will consider this quantity in a future work on rheology of this complex fluids. Lighthill has shown that the local velocity of a segment of the helix located at $\mathbf{s}$ is related to the force per unit length (i.e., Stokeslet strength) along the filament $f_\perp(\mathbf{s})$ by:

$$\mathbf{u}(\mathbf{s}) = \frac{\mathbf{f}_\perp(\mathbf{s})}{4\mu} + \int_{|\mathbf{r_0}(\mathbf{s}',\mathbf{s})|>\delta} \mathbf{f}(\mathbf{s}') \cdot \mathbb{J}(\mathbf{r_0}) d\mathbf{s}' \tag{3}$$

Where $\delta = a\frac{\sqrt{e}}{2}$ is "the natural cutoff ", $\mathbf{r_0}$ is the position vector from the point $\mathbf{s}$ on the centerline relative to the point $\mathbf{s}'$, and $\mathbb{J}$ is the Oseen tensor given by

$$\mathbb{J}(r) = \frac{1}{8\pi\mu}\left(\frac{\mathbb{I}}{|\mathbf{r}|} + \frac{\mathbf{r}\mathbf{r}^{\mathbf{T}}}{|\mathbf{r}|^3}\right) \tag{4}$$

### 3.1 Resistive Force Theory

The application of the slender body theory is important to the prediction and understanding of swimming propulsion. Now we have to find the force and torque resulting for the movement of the flagellum. This can be done by performing an integration of all the forces and torques of each small segment.We consider the force acting by an element $ds$ on the fluid is given by $\mathbf{f} = K \cdot \mathbf{u}dx$, where $\mathbf{u}$ is the local velocity and $K$ is the resistance tensor per unit length of a filament element, depends only on the geometry of the filament element and can be written as:

$$K = C_n\mathbb{I} + (C_t - C_n)\hat{t}\hat{t} \tag{5}$$

The total force exerted on the fluid by the flagellum is then:

$$\mathbf{F} = \int K \cdot \mathbf{u}ds \tag{6}$$

The total torque exerted on the fluid by the flagellum is then:

$$\mathbf{T} = \int \mathbf{r} \times K \cdot \mathbf{u}ds \tag{7}$$

with $\mathbf{u}(\mathbf{x})$ is the filament velocity, and $ds$ is the segment length how. Integrating in the contour we obtai:

$$F_y = (-\Omega R)(C_n - C_t)\sin\theta\cos\theta\frac{L}{\cos\theta} \tag{8}$$

and the torque :

$$T_y = (-R^2\Omega)(C_n\cos^2\theta + C_t\sin^2\theta)\frac{L}{\cos\theta} \tag{9}$$

In order to determine the propulsive forces and torques exerted on the swimming by the viscous fluid propulsion of different types of flagella, Gray and Hancock (1955), James Lighthill (1976) related propulsive coefficients.

## 4. RESULT AND DISCUSSION

### 4.1 EXPERIMENTAL RESULTS

Propulsive linear and angular velocity was measured using the methodology described in the second section. Range of averaged frequency, linear and angular velocity of the flagellum for the three types of helical tail are shown in table 2.

| Types | $(f)$[Hz] | $(U)$ [mm/s] | $(\omega)$[rad/s] | $F$[mN] | $T$[Nm] |
|---|---|---|---|---|---|
| Type 1 | $1.83 - 7.33$ | $0.035 - 0.116$ | $11.53 - 46.12$ | $52.92 - 57.04$ | $0.084 - 0.99$ |
| Type 2 | $2.44 - 8.56$ | $0.041 - 0.145$ | $15.35 - 53.8$ | $31.36 - 36.75$ | $0.105 - 0.114$ |
| Type 3 | $2.88 - 9.25$ | $0.052 - 0.207$ | $17.84 - 58.1$ | $23.52 - 28.32$ | $0.11 - 0.127$ |

Table 2. Experimental data: frequency, propulsion velocity and flagellum angular velocity, propulsive force and torque.

These experimental results vary linearly with external DC voltage ($V = [0, 75 - 4, 5]Volt$) supplied for the helix in the silicone oil. Fabricated prototype single rigid helix was rotated with different frequency then engine speed is diferent for the three propellers.
The uncertainty of the DC power is the uncertainty of the voltage source is given by the manufacturer and is equal to $0.01$. For the other parameters the uncertainty was calculated from a set of measurements. For the frequency we find $0.04$, for linear and angular velocity the uncertainty it is approximately 2 percent. The highest values of velocity of the swimmers $0.207mm/s$ using this value we find $Re = 0.0301$. This Reynolds number does not characterize a real micro-organism or bacteria, because they swim with Reynolds in the range of $Re = 10^{-4}$, but that number is very significant to design and carried out of the experiment in the present work. Average linear velocity is 28 percent lower with the flagellum helix 1 ($\lambda/R = 0.40$) than the flagellum helix 2 ($\lambda/R = 2.27$) and 34 percent than the flagellum helix 3 ($\lambda/R = 5$). But flagellum with helix 2 ($\lambda/R = 2.27$) have average linear Velocity 38 percent lower than helix 3 ($\lambda/R = 5$). Then to the angular velocity the results are similarvelocity is 29 percent lower with the flagellum helix 1 ($\lambda/R = 0.40$) than the flagellum helix 2 ($\lambda/R = 2.27$) and 41 percent than the flagellum helix 3 ($\lambda/R = 5$). However flagellum with helix 2 ($\lambda/R = 2.27$) have average angular velocity 19 percent lower than helix 3 ($\lambda/R = 5$). The propulsive thrust and torque produced by each helical tail is obtained using the method described in Section 2.1 and the average values are shown in Table 2. The helical with helix 3 ($\lambda/R = 5$) provide the highest thrust at $0.057N$ while the helix 1 ($\lambda/R = 0.4$) provide the smallest thrust $0.028N$. However for the torque the helical with helix 1 ($\lambda/R = 0.4$) provide the highest torque at $0.0174Nm$ while the helix 1 ($\lambda/R = 5$) provide the smallest thrust $0.099Nm$. The results of force and torque have uncertainties 3 percent.

A natural question is why a helix show different results than other helix. Considering the kinematics of the flagellum, the most relevant parameter is the number of turns N directly associated to the wavelength of the flagellum. Angular and linear velocity greater are reached when the wavelength is high, that mean helix 3 presents kinematic characteristic higher than the other helices. Now considering the dynamics of the flagellum the parameter most relevant is the radius of the helix. If the helix radius increases the force exerted on the fluid increases because the interactions between the flagellum and the fluid increase. This explain why helix 1 has greatest force and torque than the other helix 2 and helix 3. So we proved again a decrease in the size of the body of the flagellum result in increment of velocity. The propeller introduced into viscous fluid have complex kinematic and dynamic processes.

The experimental hydrodynamic force is presented as a function of the immersion of the length of the propeller in the fluid and the velocity V in which the propeller is immersed influenced by the frequency of the motor, this parameters also affect the flow and the results. For a real bacteria Liu et al. (2011) show relevant results in the design of micro-robots, as they indicate the length of a maximum speed at which they can swim. Acording a relation between force and velocity, it can be observed that for a slow speed, the hydrodynamic force is lower corresponding to the thrust for a high speed the hydrodynamic force is higher corresponding to the thrust. The results obtained here are in agreement with other experimental works developed by Rodenborn (2011), and Akanksha (2018). An interesting activity would be an experimental analysis to understand and collaborate with the prediction of the free swimming condition of micro-organisms and micro-robots, and the hydrodynamic forces and torques generated by the propulsion of flagella. most of the results for the three helix will be different for a areal micro-organism, but it can be used for comparison or used for practical application such as Drug delivery or Minimally Invasive Surgery.

The flagellum of the present work a have a frequency and involves oscillating flow, the creeping flow equation is ensured since $Re << 1$ and $Sh \times Re << 1$. Here $Sh$ is the Strouhal defined as $Sh = 2\pi fR/U$. figure 4 and 5 shows Non-dimensional force induced by the flagellum in the fluid as a function of the Strouhal number for three differentes helix conditions. Dimensionless force and torque are obtained dividing by $\mu\omega R^2$ and $\mu\omega R^3$ respectively experimental force and torque.

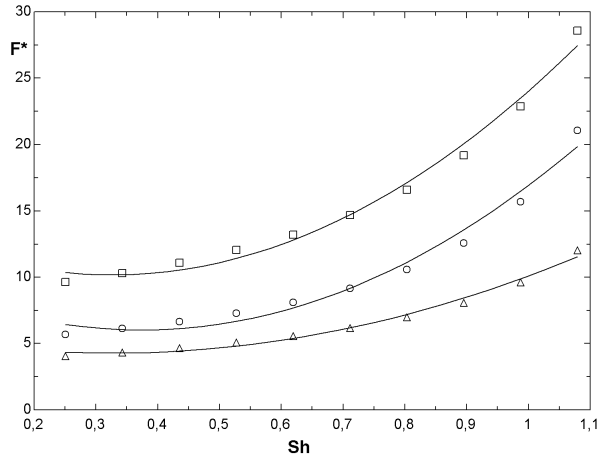


Figure 4. Non-dimensional force induced by the flagellum in the fluid as a function of the Strouhal number for three differentes helix condtions, helix 1 (rectangle), helix 2 (circle), helix 3 (triangle).

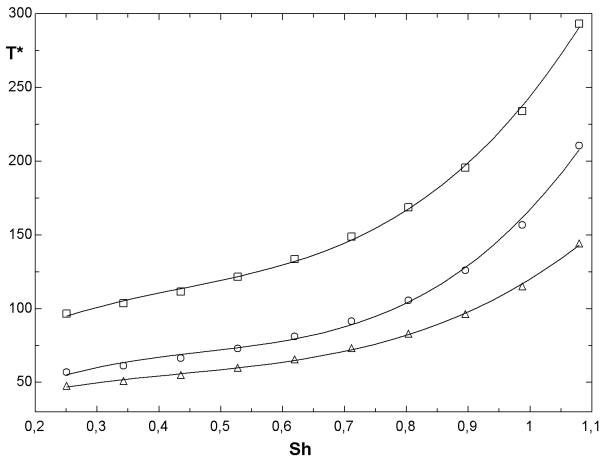


Figure 5. Non-dimensional torque induced by the flagellum in the fluid as a function of the Strouhal number for three differentes helix conditions, helix 1 (rectangle), helix 2 (circle), helix 3 (triangle).

The Reynolds number $Re$ is calculated using propulsive linear velocity and the radius of each helix. The normalized force and torque produced by the three prototypes inf unction of the Reynolds number is shown in figure 4 and 5. The resistive force theory suggests that the hydrodynamic forces are linearly proportional to the fluid viscosity, and thus inversely with the Reynolds number. Result from our experiment are in agreement with the theory.

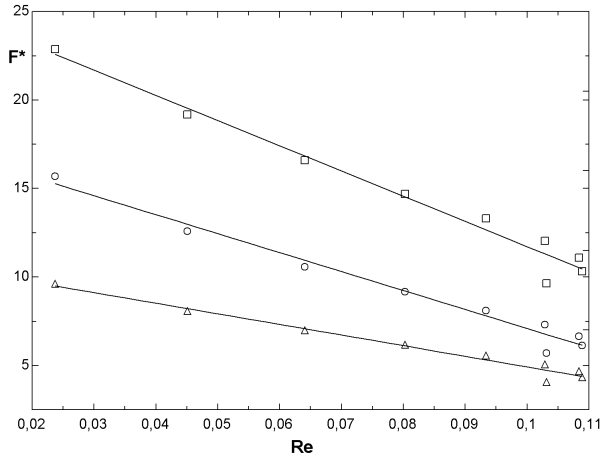


Figure 6. Non-dimensional force induced by the flagellum in the fluid as a function of the Reynolds number for three differentes helix condtions, helix 1 (rectangle), helix 2 (circle), helix 3 (triangle).

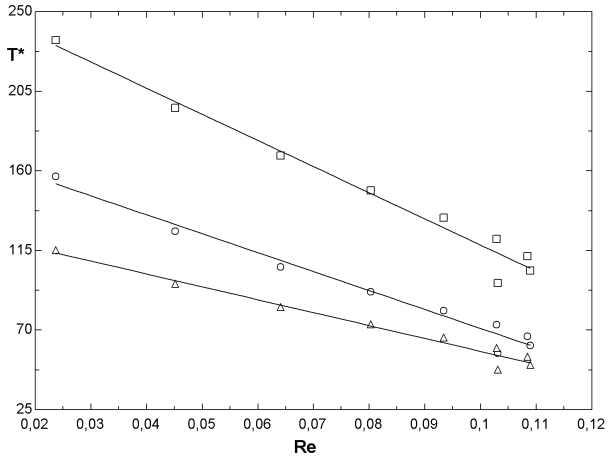


Figure 7. Non-dimensional torque induced by the flagellum in the fluid as a function of the Reynolds number for three differentes helix condtions, helix 1 (rectangle), helix 2 (circle), helix 3 (triangle).

### 4.2 NUMERICAL RESULTS

The most commonly used expression for resistive force theory are used in the present work. The expression for $C_n$ and $C_t$ respectively are presented in table 3. Here a is the filament radius, R denotes the helix radius. $L$ is the full length of the flagellum and $\lambda$ the wavelength of the micro-organism flagellum during its motion. Resistive force theory predicts the thrust, torque, by an integration of the force and torque from each small segment as describe in the first section.

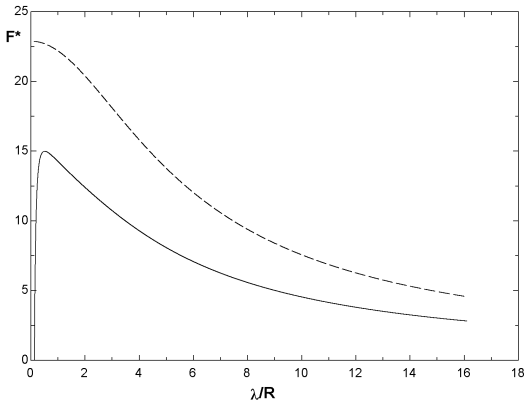


Figure 8. Nondimensional force as a function the non-dimensional wavelength, Lighthill RST (dotted line), Gray and Hancock RST (continuous line).

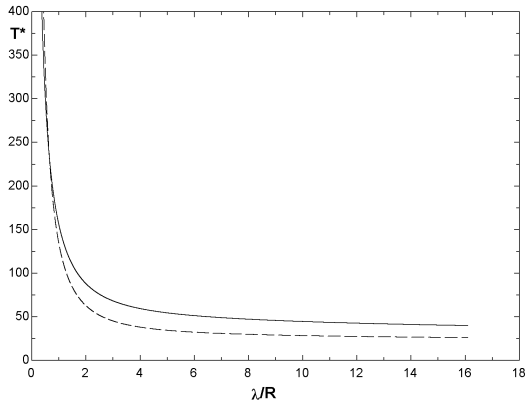


Figure 9. Nondimensional torque as a function non-dimensional wavelength,Lighthill RST (dotted line), Gray and Hancock RST (continuous line).

A program in Matlab is provided,for calculating force, torque for the helical flagellum. The program takes as input the parameters for helical flagellum $[R, L, a, \lambda]$. The helical radius $R$ is used as the unit of length in the program. Figures 8 and 9 show the results for force and torque on the micro-organism as a function of non-dimensional wavelength $\lambda/R$ using both Lighhill resistive force theory and Gray and Hancock theory. Force is dimensionless dividing by $\mu\omega R^2$ and torque is dimensionless dividing by $\mu\omega R^3$. It is seen that both force and torque decay as the wavelength of the flagellum increase. The result based on Gray and Hancock model predicts a maximum force $F_{max} = 14.98$ at $\lambda/R = 0.943$. Whereas figure 8 shows a high discrepancy between the theories investigated. The torque is found to be in a very goods agreement as the wavelength goes to zero. However, there is a significance difference between the torques predicted by the theories for $\lambda/R > 2$. We can see in figure 9 for the both theoretical predictions the torque are very close, while for the force in figure 8 the Lighthill prediction is overestimated in relation to the Gray theory. The predictions of the force and torque seems to work consistently. It is seen that the drag model coefficient based on Gray an Hancock (1955) gives a smaller force than the Lighthill (1976).

Is important to note the drag coefficients specified in classical RFT assume an infinite flagellum length and do not put the time-dependent complex periodic flow structures at the ends of the flagellum. Is the Limitation of Resistive Force Theory (RFT) Predictions. But our study shows that the propulsive performance of flagella helix systems can be reliably predicted by traditional RFT although that does not consider the complex interactions between the phase-angled flagella units for the $Re$ and $Sh$ range investigated. In the next section we compare experimental and numerical results.

Note that the zero-thrust condition implies that the torque generated by the fagellum it is cancelled out by the drag that is produced only by it, without considering the effect of the drag produced by the head (Lighthill, 1996a). For helical propulsion at zero-thrust condition, the axial velocity decays exponentially with the distance from the helical axis. Other author also analysed,the zero-thrust condition by helices of infinite length. Johnson (1980) applied direct numerical calculations to solve the RST and considering that the helices can translate along its centre of symmetry and rotate with and specify angular velocity. A better approximation common used is the method of regularized Stokeslets (MRS). Is a method that represents the fluid velocity in Stokes flow by a collection of regularized forces. Cutoff functions are introduced to regularize the singular fundamental solutions known as Stokeslets. This regularization removes the singular nature from the velocity field, hence the velocity can be evaluated anywhere in the fluid, including at the location of a regularized Stokeslet. There exists a linear relationship between regularized Stokeslet forces and the velocity anywhere in the fluid. Hence, regularized Stokeslets strengths can be computed to impose velocity constraints at a collection of points in the flow. In the particular application of interest, the velocity constraints correspond to the motion of an immersed boundary in the flow. The regularized Stokelest method result only depend on the choice of the parameter $\epsilon$. We will consider this mehod in furure work.

| Cn | Ct | Author |
|---|---|---|
| $\frac{4\pi\mu}{ln(2\lambda/a)+0.5}$ | $\frac{2\pi\mu}{ln(2\lambda/a)-0.5}$ | Gray and Hancock (1955) |
| $\frac{4\pi\mu}{ln(0.18\lambda/a\cos\theta)+0.5}$ | $\frac{2\pi\mu}{ln(0.18\lambda/a\cos\theta)}$ | James Lighthill (1976) |

Table 3. Drag coefficients used in literature

Dimensionless propulsive velocity is plotted in figure 10, adimensionalization is done by dividing the velocity by $\omega R$. In addition, $V/\Omega R$ measures the importance between the propulsion movement and the rotational movement of the flagellum.

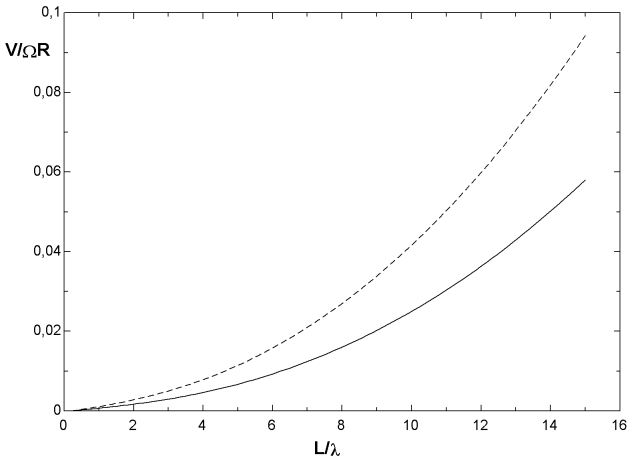


Figure 10. Dimensionless propulsive velocity as function of $L/\lambda$, Lighthill RST (dotted line), Gray and Hancock RST (continuous line).

### 4.3 COMPARISON OF EXPERIMENTAL RESULTS WITH RESISTIVE FORCE THEORY

Finally we compared our experiment data with the predictions from the slender body theory. In figure 11 we can see the results from resistive force theory and the experiment are shown with black circles. We found that the dimensionless force of the bacterium when ($\lambda/R = 0.4$) is within 11 percent lower than the prediction by Lighthill, and 31 percent smallest than the Gray and we concluded that the experimental results are better represented by the Lightill. Also we found too the results from resistive force theory and the experiment for the helix 2 where ($\lambda/R = 2.7$) is within 14 percent lower than the prediction by Lighthill, and 28,7 percent higher than the Gray. And for the helix 3 where ($\lambda/R = 5$) the experimental result is within 31,25 percent lower than the prediction by Lighthill, and 18,2 percent higher than the Gray, in this case Theory from Gray give better approximation.

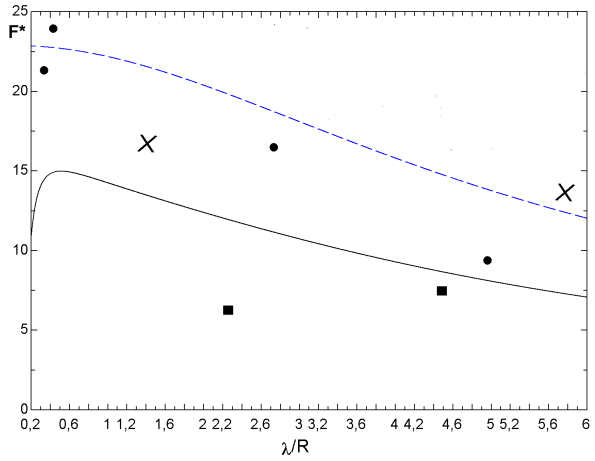


Figure 11. Experimental point and prediction force by RST for the flagellum, Lighthill RFT (dotted line), Gray and Hancock RFT (continuous line), experimental this work (black circle),experimental Rodenborn (black rectangle), experimental Akanksha (x)

Using these experimental results, we can now make a comparison between experimental and numerical results for the propulsive torque of the flagellum. Figure 12 shown along with the predictions from resistive force theory. Experimental

and numerical results are in excellent agreement, generally agreeing within 3 which demonstrates the accuracy of both our experiments and the theories.

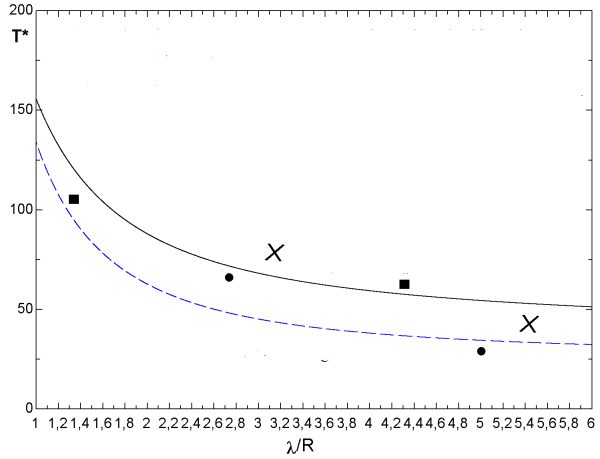


Figure 12. Experimental point and prediction torque by RST for the flagellum, Lighthill RFT (dotted line), Gray and Hancock RFT (continuous line), experimental this work (black circle),experimental Rodenborn (black rectangle), experimental Akanksha (x).

## 5. CONCLUSIONS

In this paper experimental and theoretical analysis was presented for a macroscopic model of helical flagellum.Three different helices is used for these experiments and we do measurement for propulsive velocity, induced angular velocity as well as propulsive thrust and torque exerted by the rotating helix in a highly viscous fluid. Experimental results vary linearly with external DC voltage. We use resistive-force theory in order to compare experimental results with those predicted by literature. A very good agreement quantitative was observe and theoretical predictions for propulsive force and torque diverge poorly. We can minimize this divergence,considering the uncertainty in the experimental measurement are less than 10 percent.

## 6. ACKNOWLEDGEMENTS

This work was supported by CAPES and VORTEX-UNB

## 7. REFERENCES

Akanksha, T. and Manesh, T 2018. " Trajectory of a model bacterium" J Fluid Mech 10.1017-2017.758

Gray, J. and Hancock, G. J. 1955. "The propulsion of sea-urchin spermatozoa". J. Exp. Bio 32 (4), 802–814.

Johnson, R. E 1980 "An improved slender-body theory for stokes flow". J Fluid Mech 99: 411–431.

Kim S and Karrila J.S 1991."Microhydrodynamics:Principles and Selected Applications" (Boston: Butterworth-Heinemann)

Koch D.L 2011. "Collective hydrodynamics of swimming microorganisms: living fluids" Annu Rev Fluid Mech 43,637-659

Lighthill, J. 1976."Flagellar hydrodynamics". The John Von Neumann lecture. SIAM Review 18 (2), 161–230.

Liu. B, T. R. Powers, and K. S. Breuer, 2011. "Force-free swimming of a model helical flagellum in viscoelastic fluids". Proceedings of the National Academy of Sciences, 108(49), 19516-19520. doi: 10.1073/pnas.1113082108.

Nelson, B.J and Kaliakatsos K.I and Abbott, J.J "Microrobots for minimally invasive medicine," Annual Review of Biomedical Engineering, Vol.I2, pp.55-85, 2010.

Rodenborn, B. Chen, C.-H. Swinney, H. L., Liu, B. Zhang, H. P. 2013. "Propulsion of microorganisms by a helical flagellum". Proc. Natl. Acad. Sci. 110 (5), 338–347 .

Sznitman,J. and Shen, Sznitman, R. and Arratia, P.E "Propulsive force measurements and flow behavior of undulatory swimmers at low Reynolds number," Physics in Fluids, Vol.22, pp.I2190 1, 2010.